Impact Factor (SJIF): 2.125

International Journal of Advance Research in Engineering, Science & Technology

e-ISSN: 2393-9877, p-ISSN: 2394-2444

Volume 3, Issue 1, January-2016

EXPERIMENTAL AND NUMERICAL ANALYSIS OF AN CRACKED ADHESIVE JOINT

Jay Mandaliar[1], Prof. R. B. Barjibhe[2]

[1] Department of Mechanical Engineering, S.S.G.B.C.O.E.T, Bhusawal, jaymandalia@gmail.com
[2] Department of Mechanical Engineering, S.S.G.B.C.O.E.T, Bhusawal, rahulbarjibhe@yahoo.

Abstract

Adhesive bonding is a viable alternative to traditional joining systems (e.g., riveting or welding) for a wide class of components belonging to electronic, automotive, and aerospace industries. However, adhesive joints often contain flaws; therefore, the development of such technology requires reliable knowledge of the corresponding fracture properties. This study deals with ideology to obtain a specific load-displacement relationship based on the problem for PMMA/Epoxy adhesive joint along with maximum stress calculations, on Mode-I conditions. The experimental results are validated using numerical finite element analysis tool as Ansys Workbench 15.0. This information is valuable for predicting the durability of a structure containing adhesively bonded joints.

Keywords*-adhesive joints, fracture, load-displacement analysis, mode-I failure, Ansys Analysis.*

I. INTRODUCTION

With the increasing demands from the customers and industry, it is required to stimulate new technology. For instance, in Automobile sector, the present scenario is increasing light weighted technology with maintaining the standards in emission and failure criterions. When it comes to joints, this light weighted combination is required to be joined with high strength low cost materials. These materials are known as adhesives, which, adds little wright to the structure and combination of joining even two dissimilar metals and non-metals is possible which is not possible even with welded joints. The use of adhesive joints in automotive, aerospace, biomedical, and microelectronics industries is widespread; however, inaccurate joint fabrication or inappropriate curing may cause the presence of bubbles, dust particles or un-bonded areas in the bond line. As a result of which it is mandatory to assess the reliability of this adhesive joints in events of fracture in order to avoid an accident. For the study, pre-cracked specimens are used with pre-crack length of 15 mm and 25 mm.

II. LITERATURE SURVEY

Hutchinson and Suo, a practical approach for characterizing the adhesion of polymer coatings to metal substrates is to use sandwich specimens, which can be analyzed using interfacial linear elastic fracture mechanics (LEFM) concepts. ***Wang,*** however, there can be limitations to the use of LEFM in sandwich structures. The first is that the assumed stress fields are not rigorously correct, for example, in the case of large-scale plasticity or in the case of very thin layers where the K-dominant field cannot develop. ***Li et al.,*** the second is that some joints may not have macroscopic defects large enough to be considered cracks for the purpose of fracture mechanics. ***Dugdale and Barenblatt,*** these issues can compromise the utility of LEFM and alternative approaches must be sought. Cohesive zone modeling is one such approach. The key concept of cohesive zone modeling is that the failure process zone can be described by a traction–separation law; more specifically, the cohesive traction, $\sigma(\delta)$, can vary along the failure process zone, but only depends on the local opening, δ. The key is the introduction of a second fracture parameter, e.g., the cohesive strength, in addition to the fracture toughness. This cohesive strength relates the toughness to the critical crack-tip opening required for crack propagation. Recently cohesive zone modeling has been applied to solve interfacial fracture problems. ***Yang and Thouless,*** proposed a modified criterion for mixed-mode interfacial fracture, in which fracture occurs when the mode 1 and mode 2 energy release rates for the cohesive zone reach a critical value. Nevertheless, in both criteria, with independently characterized mode 1 and mode 2 traction–separation laws available, mixed-mode problems with a range of fracture mode-mixes can be fully solved. ***Swadener and Liechti*** examined cohesive zone modeling for a wide spectrum of interface problems, such as glass/epoxy interfacial fracture and adhesion.

Cotterell and Mai; Pandya and Williams, one is through direct tension or shear experiments, however, in these experiments, the damage evolution across the width of the specimen must be uniform, which is usually difficult to achieve. ***Li et al.,*** in the second approach, the cohesive law is derived from simultaneous measurements of the J-integral and the end-opening (both normal and shear) of the cohesive zone. This has been successfully employed in the extraction

of traction–separation laws for cementitious components. ***Sorensen***, successfully employed the same for adhesive bonds while, ***Sorensen and Jacobsen,*** employed the approach for fiber-reinforced composites.

III. ADHESIVE JOINTS.

3.1 Application.

The material combination that has been selected is PMMA/Adhesive. Poly methyl methacrylate has wide number of industrial application, such as,

1. Automotive Industry
2. Marine Applications
3. Aviation Industry
4. Electronic Components
5. Interiors and Furniture
6. Architecture and Construction.

Polyurethane material (Loctite MS 930) is selected as an adhesive in order to obtain the required bonding between PMMA Blocks.

IV. EXPERIMENTAL WORK

The double cantilever beam (DCB) configuration was used to determine the mode 1 load–separation laws. [1] The specimen geometry is shown in Fig. 4.1. A pre-existing crack in the middle of the adhesive layer was cut using a sharp razor blade of 05mm, 15mm and 25mm for respectively two specimens.

4.1 Specimen Preparation: [1]

The specimens were manufactured in two different ways.

- Method (1): The two plates with applied adhesive are cured. After the curing process, specimens are cut from the plates.

The specimens for measuring the unconfined tensile behaviour of the PU bond were obtained from thin films. In this case, the PU fluid was applied on top of a PMMA block to form a thin film with thickness of 5 ± 0.1 mm.

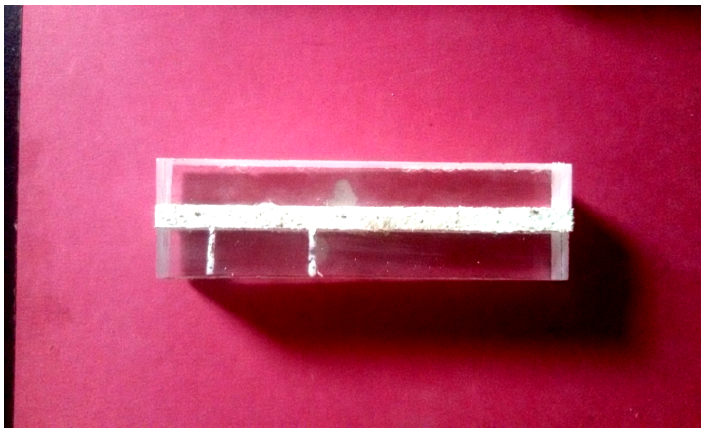

Figure 4.1: Actual DCB test configuration and specimen

Table 4.1 Dimension of Specimen Geometry

Sr. No.	Material	Length (mm)	Width (mm)	Height (mm)
1	PMMA	90	20	10
2	ADHESIVE	90	20	05

4.2 Testing of Specimen:

The most straightforward method to test adhesives was to use a test specimen made entirely of the adhesive material. When extracting constitutive relations from experiments on a thin film adhesive it is of utmost importance to know the stress distribution in the test specimen. As mentioned earlier, the stress distribution relies highly on the geometry of the specimen. The specimen as shown in fig 4.1 were prepared and tested on the universal testing machine. The required date

was collected, such as maximum stress, maximum strain, the graph of load vs. displacement and the cohesive law has been derived from it.

Figure 4.2: Universal Testing Machine used for Testing

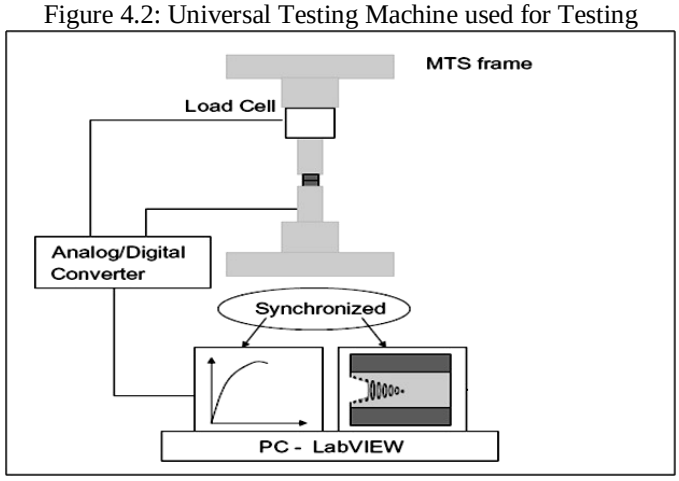

Figure 4.3: Schematic of experimental set-up [1]

All the experiments were conducted at room temperature using a load cell based materials testing system under constant crosshead speed. The material testing system used in the experimental work is a Universal Testing Machine with 10 KN Capacity and an accuracy of ± 1%. The differences noticeable under tensile loading and reliance on crosshead displacements would clearly lead to low measurements of moduli. In all total six experiments were conducted for the same samples with different openings as 2 samples of 05 mm opening, at the constant loading rate of 0.3 mm/s. [1]

4.3 05mm Pre-cracked Experimental Specimens.

Table4.2 Experimental Results of 05mm Specimens

Sr. No.	Specimen No.	Max. Disp. δ mm	Max. Force, N	Max. Stress. σ MPa
1	1	11.4	331.24	3.31
2	6	17.1	326.24	3.26

Graph 4.1: Load Profile for 5mm Pre-cracked Specimens

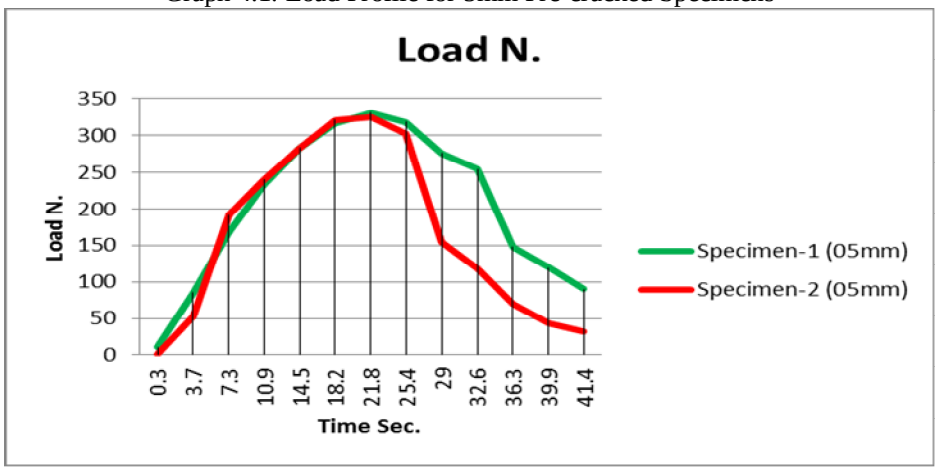

4.4 15mm Pre-cracked Experimental Specimens.

Table4.3 Experimental Results of 15mm Specimens

Sr. No.	Specimen No.	Max. Disp. δ mm	Max. Force, N	Max. Stress. σ MPa
1	2	15.1	234.22	2.34
2	5	13.9	229.34	2.29

Graph 4.2: Load Profile for 15mm Pre-cracked Specimens

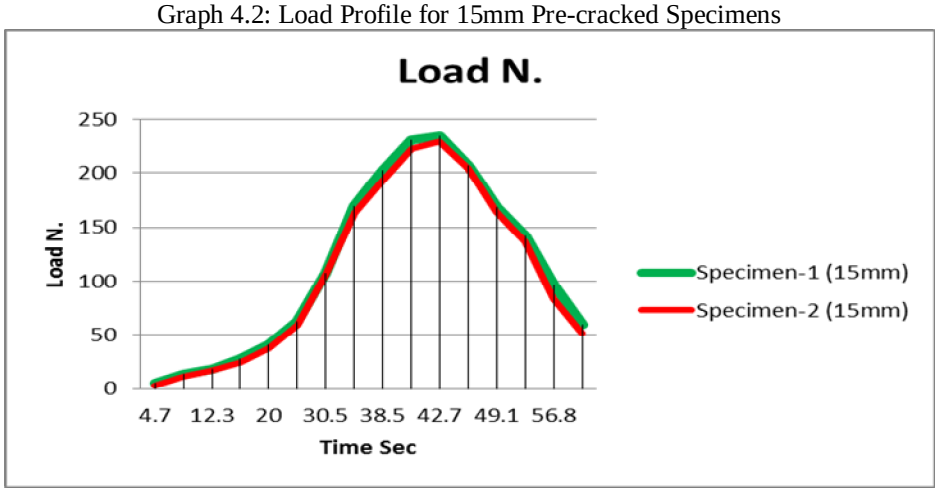

4.5 25mm Pre-cracked Experimental Specimens.

Table4.4 Experimental Results of 25mm Specimen

Sr. No.	Specimen No.	Max. Disp. δmm	Max. Force, N	Max. Stress. σ Mpa
1	3	17.2	141.12	1.41
2	4	8.7	164.64	1.64

Graph 4.3: Load Profile for 25mm Pre-cracked Specimen

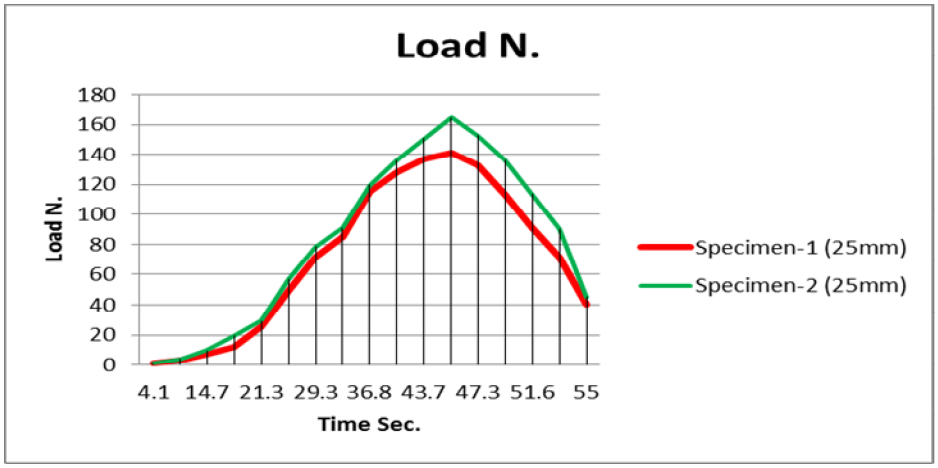

Fig.4.5 Failure Sequence of the specimen

V. NUMERICAL ANALYSIS

For the numerical analysis Ansys workbench 15.0 was used as FE tool. Simple two dimensional element was consider with pre-cracked geometry of 5mm, 15mm, and 25mm pre-cracked structures respectively in order to analyze the behavior of the joint.

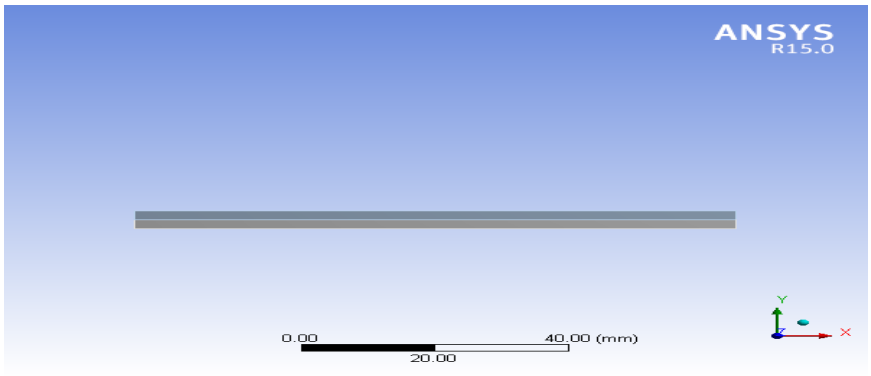

Figure 5.1: Specimen Geometry from Ansys.

Table 5.1: Material Property of Body Material

Material Properties of Body Material	
Young's Modulus X direction MPa	1.35E+05
Young's Modulus Y direction MPa	9000
Young's Modulus Z direction MPa	9000
Poisson's Ratio XY	0.24
Poisson's Ratio YZ	0.46
Poisson's Ratio XZ	0.24
Shear Modulus XY MPa	5200
Shear Modulus YZ MPa	1.00E-04
Shear Modulus XZ MPa	1.00E-04

Table 5.2: Property of CZM Material

Material Properties of CZM Material	
Maximum Normal Contact Stress MPa	110
Critical Fracture Energy for Normal Separation mJ mm^-2	182.76
Maximum Equivalent Tangential Contact Stress MPa	1.00E-36
Critical Fracture Energy for Tangential Slip mJ mm^-2	1.00E-33
Artificial Damping Coefficient s	1.00E-08

5.1 05 mm Pre-cracked Specimens.

The directional deformation, total deformation stresses are explained here.

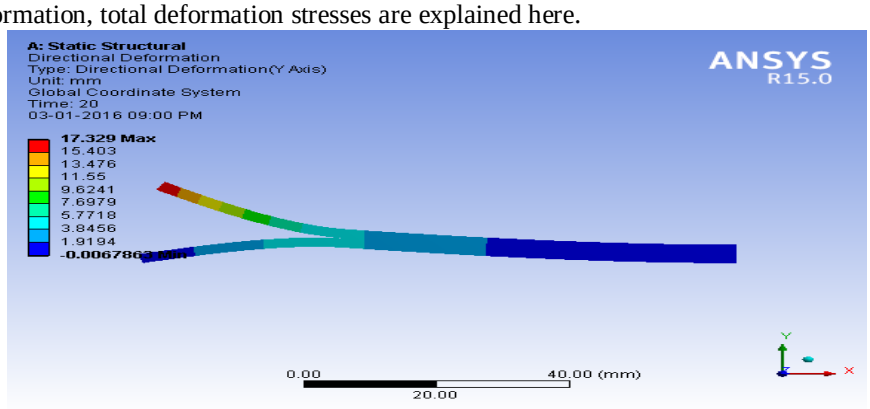

Figure 5.2 Directional Deformation of 05mm Specimen

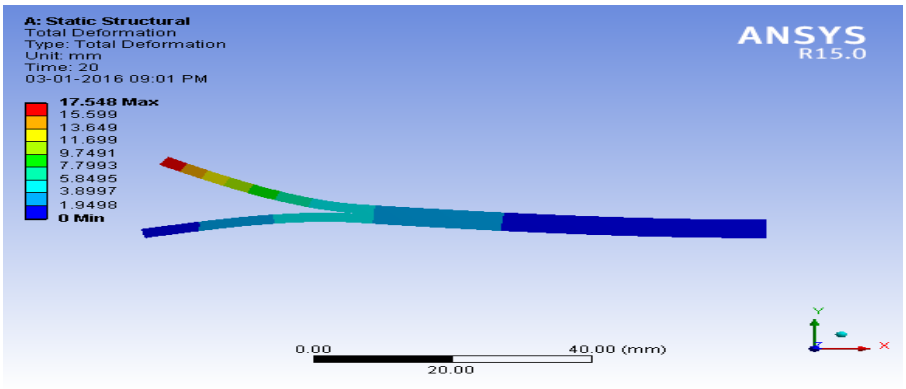

Figure 5.3 Total Deformation of 05mm Specimen

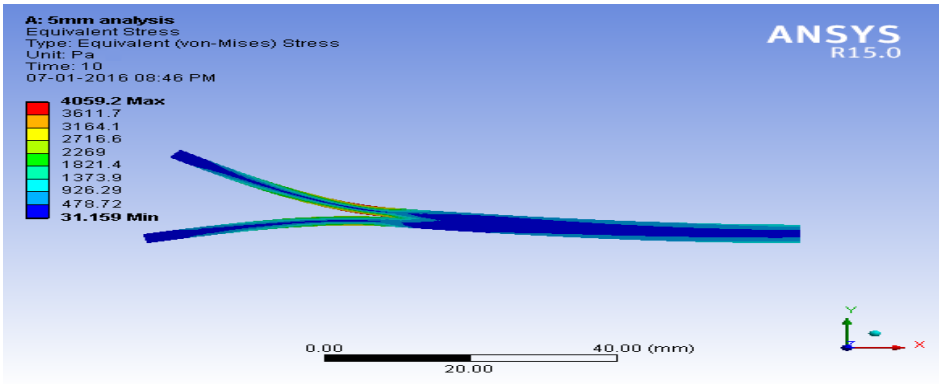

Figure 5.4 Stresses of 05mm Specimen

5.2 15 mm Pre-cracked Specimens.

The directional deformation, total deformation stresses are explained here.

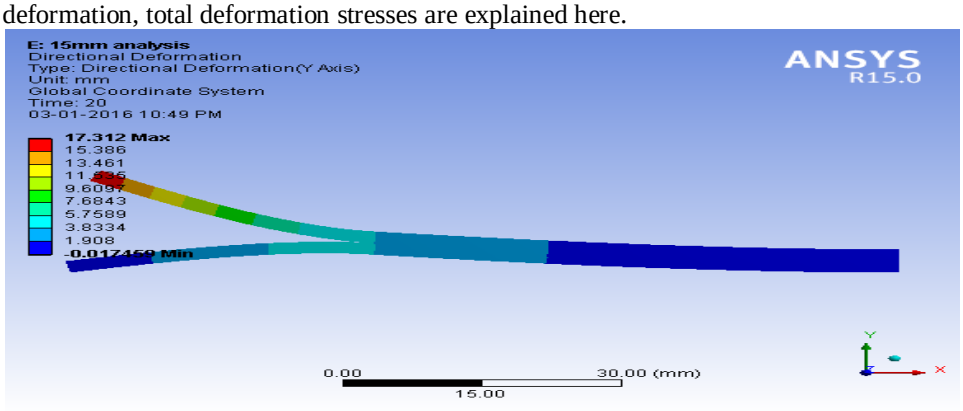

Figure 5.5 Directional Deformation of 15mm Specimen

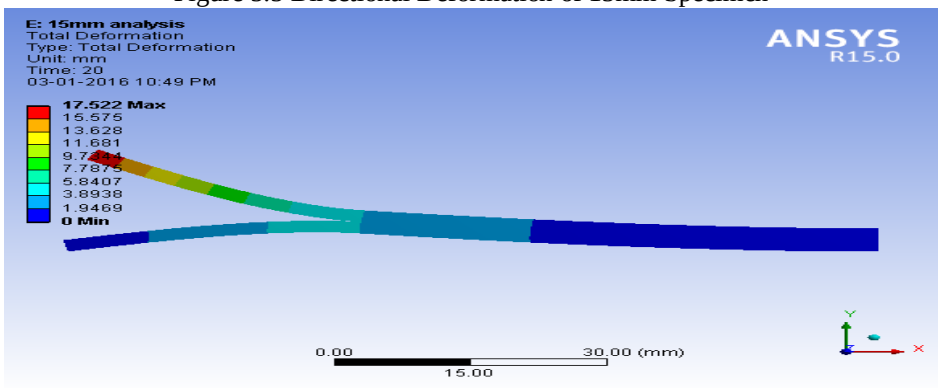

Figure 5.6 Total Deformation of 15mm Specimen

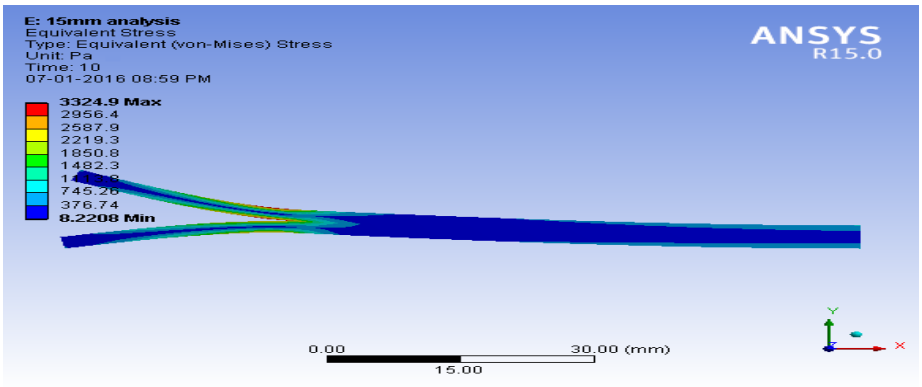

Figure 5.7 Stresses of 15mm Specimen

5.3 25 mm Pre-cracked Specimens.

The directional deformation, total deformation stresses are explained here.

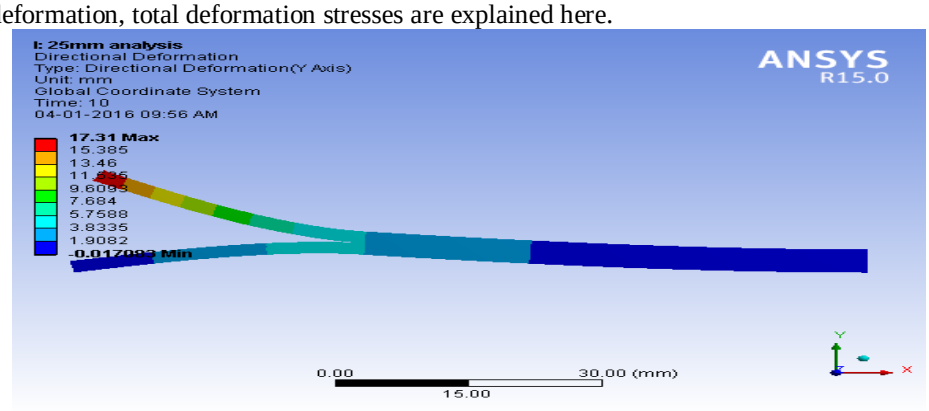

Figure 5.8 Directional Deformation of 25mm Specimen

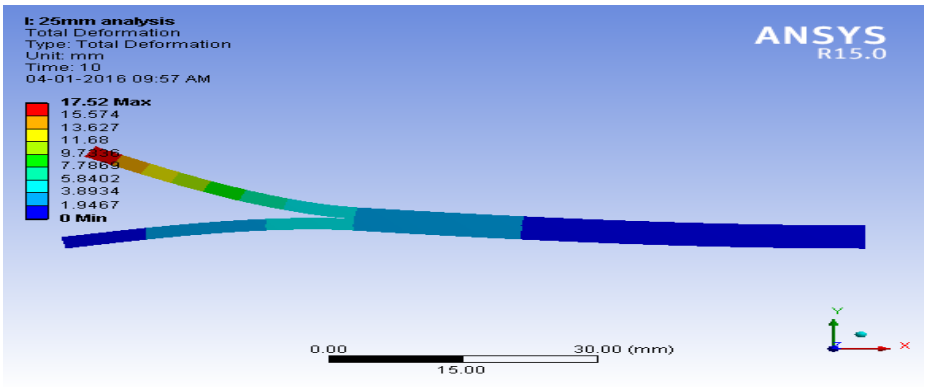

Figure 5.9 Total Deformation of 25mm Specimen

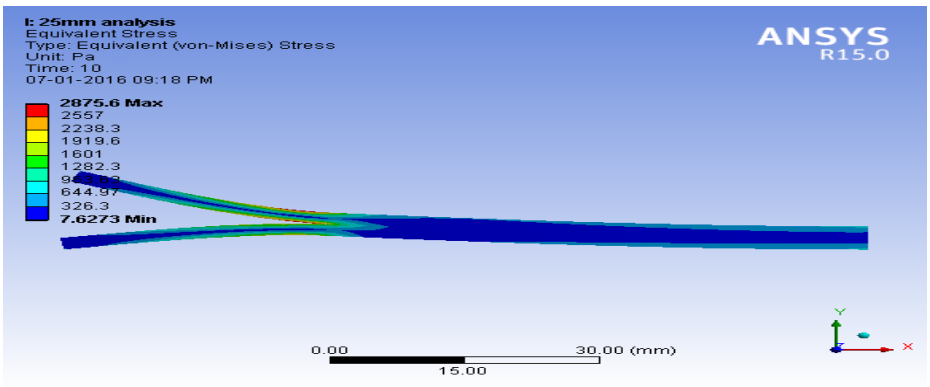

Figure 5.10 Stresses of 25mm Specimen

Table5.3 Results of Numerical Analysis

Sr. No.	Specimen	Max. Load N.	Stresses, MPa
1	5mm	337.38	3.726
5	15mm	220.71	2.616
9	25mm	160.82	1.875

VI. RESULTS AND DISCUSSION

The experimental testing was done at room temperature using standard testing conditions. The results obtained from experimental and Ansys formulations are as explained below.

6.1 ANALYSIS OF 5MM PRE-CRACKED SAMPLES.

6.1.1 Load Analysis.

Table 6.1: Load Comparison between Experimental Results and Ansys of 5mm pre-cracked sample.

Sr. No	Specimen No.	Experimental Result, N	Ansys Result, N	% Error
1	1	331.24	337.38	1.81
2	2	326.24		

Graph 6.1: Load Analysis for 5mm pre-cracked specimens.

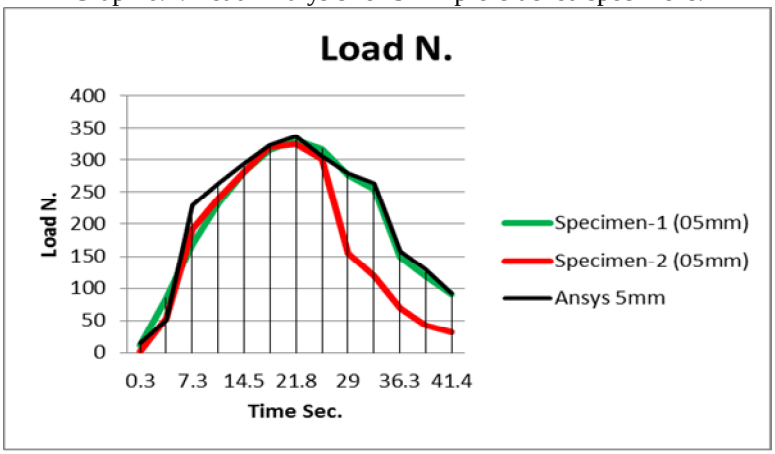

It can be clearly identified from the above data that the behaviour of the 5mm pre-cracked sample remains the same. Though little variation is seen in both the samples used for experimentation but the same variations can be accounted owing to the reason that the samples are adhesively bonded. Thus though utmost care has been taken in preparation of the samples still error has to be accounted for.

6.1.2 Stress Analysis.

Table 6.2: Stress Comparison between Experimental Results and Ansys of 5mm pre-cracked sample.

Sr. No	Specimen No.	Experimental Result, MPa	Ansys Result, MPa	% Error
1	1	3.303	3.726	10.3
2	2	3.232		

Graph 6.2: Stress Analysis for 5mm pre-cracked specimens.

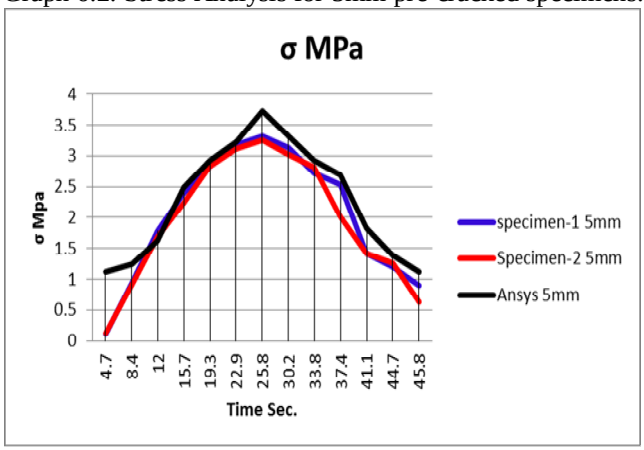

Looking at the graph it has been clear that the behaviour of experimental sample and the numerical simulation has identical profile. Still it can be seen that the maximum stress recorded experimentally was 3.303 MPa whereas on numerical simulation it was 3.726 MPa. An error or nearly 10% can be accounted for the same.

6.2 ANALYSIS OF 15MM PRE-CRACKED SAMPLES.

6.2.1 Load Analysis.

Table 6.3: Load Comparison between Experimental Results and Ansys of 15mm pre-cracked sample.

Sr. No	Specimen No.	Experimental Result, N	Ansys Result, N	% Error
1	1	234.2	220.71	3.74
2	2	229.3		

Graph 6.3: Load Analysis of 15mm pre-cracked samples.

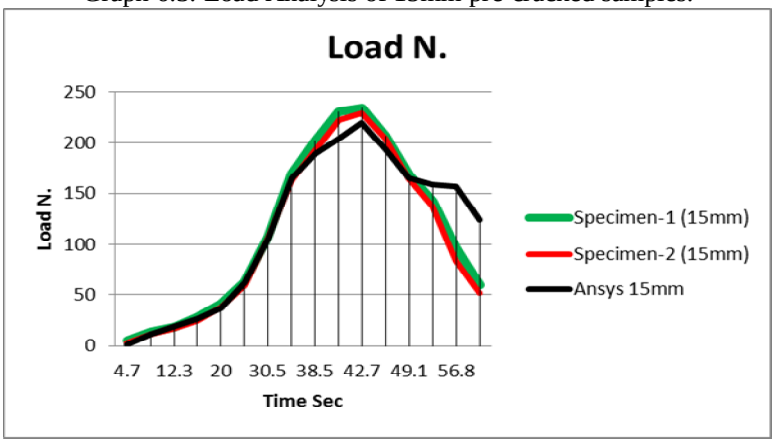

The maximum load recorded experimentally was 234.2 N whereas the same obtained from simulation in Ansys workbench was 220.71 N. comparisons shows an error of 3.74%. This result is justified.

6.2.2 Stress analysis

Table 6.4: Stress Comparison between Experimental Results and Ansys of 15mm pre-cracked sample.

Sr. No	Specimen No.	Experimental Result, MPa	Ansys Result, MPa	% Error
1	1	2.332	2.616	10.1
2	2	2.293		

Graph 6.4: Stress Analysis of 15mm pre-cracked specimen.

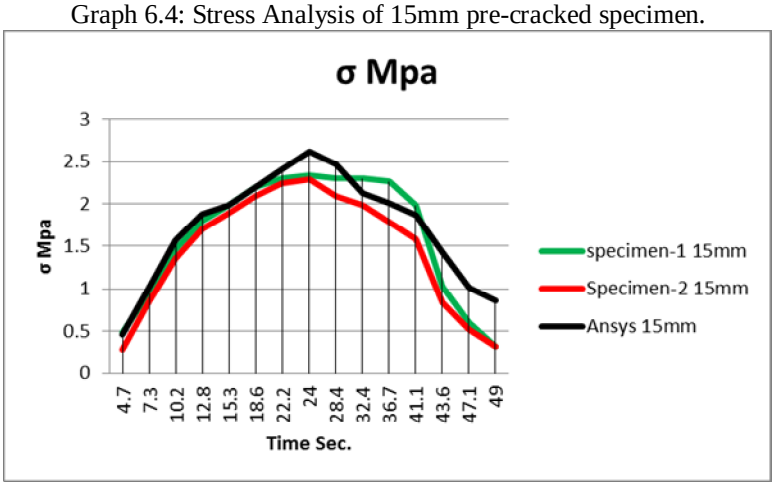

Here it can be seen that the stresses on the contrary for numerical analysis are more as compared to those recorded experimentally. The maximum value recorded experimentally was 2.332 MPa and numerically it was obtained as 2.616 MPa. The maximum recorded error is 10.1. This is because of the reason that no two adhesive joints can be identical. Manually it is not possible to apply identical amount of adhesives to every geometry. This results in error.

6.3 ANALYSIS OF 25MM PRE-CRACKED SAMPLES.

6.3.1 Load Analysis.

Table 6.5: Load Comparison between Experimental Results and Ansys of 25mm pre-cracked sample.

Sr. No	Specimen No.	Experimental Result, N	Ansys Result, N	% Error
1	1	141.12	160.82	2.32
2	2	164.64		

Graph 6.5: Load analysis for 25mm pre-cracked specimen.

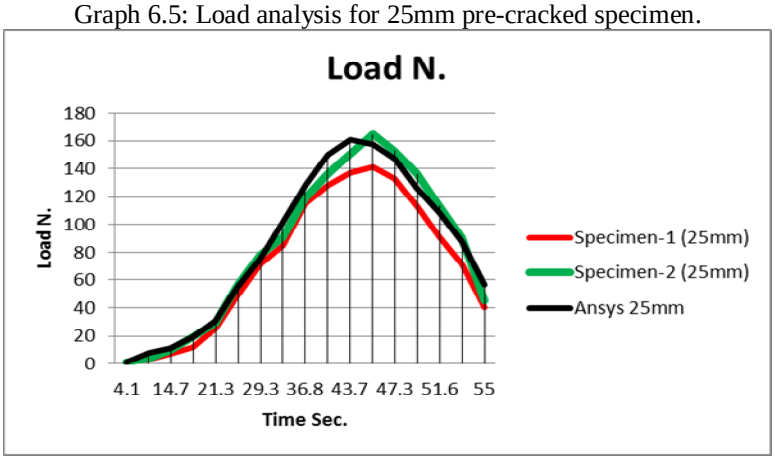

The maximum load recorded experimentally out of the two specimens was 164.64 N whereas the maximum load recorded from Ansys workbench 15.0 is 160.82 N. The working error of 2% is recorded which is within working limits.

6.3.2 Stress analysis

Table 6.4: Stress Comparison between Experimental Results and Ansys of 25mm pre-cracked sample.

Sr. No	Specimen No.	Experimental Result, MPa	Ansys Result, MPa	% Error
1	1	1.411	1.875	11.3
2	2	1.646		

Graph 6.6: Stress Analysis of 25mm pre-cracked specimen.

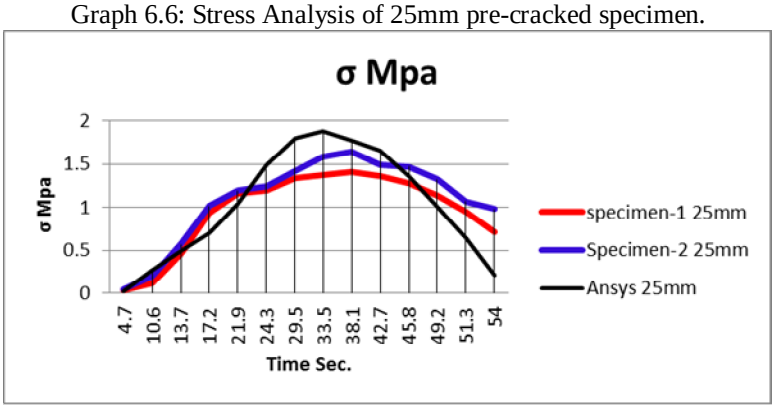

From the results obtained experimentally the maximum recorded stress was 1.646 MPa, whereas the same obtained from Ansys workbench was 1.875 MPa. The comparison of both the results shows the error of nearly 11%. Here this error is accounted for the maximum pre-cracked structure. While practical study done has results on little inferior side just because there can be shortcomings during the construction of adhesive joints.

Apart from the work done emphasis can be laid upon the various parameters in future as mentioned below.

1. Fracture Tensile Tests were carried out at one opening only. However need to be conducted over a wide range of openings.
2. Fracture Tensile Tests were conducted for one strain rate only at room temperature. However it is needed to be conducted for different displacement rates.
3. The fracture toughness studies were done at room temperature. It is suggested to conduct the test at low temperatures and elevated temperatures.
4. The material geometry is needed to be tested for Mode-II (Shear Load) and Mode-III (Mixed Mode) loading.
5. Experimental evaluation can also be done with variable loading angles in order to study the various fracture parametric behavior.
6. Fatigue crack growth studies may also be conducted applying realistic spectrum variable amplitude conditions.
7. Strain field distribution may be obtained using soft computing and CAE software under various conditions.

VI. REFERENCES.

1. Jay Mandalia, Prof. Rahul B. Barjibhe “Mode-I Traction-Separation of an Adhesive Joint” International Journal of Advance Research in Engineering, Science & Technology, Volume 2, Issue 12, December- 2015, PP - 1114-1119.
2. Jay Mandalia, Prof. Rahul B. Barjibhe “Experimental Analysis of Cracked Adhesive Joint” International Journal of Advance Research in Engineering, Science & Technology, Volume 3, Issue 1, January 2016.
3. Young Zhu, K. M. Liechti and K. Ravi-Chandar, "Direct extraction of rate dependent Traction-Separation for Polyurea/Steel Interface", ‘International Journal of Solids and Structures’, 2009, Vol. No. 46, PP 31-51.
4. Adams, R.D., Comyn, J.C. and Wake, W.C. "Structural Adhesive Joints in Engineering", Chapman & Hall, London, 1997 UK.
5. Akisanya, A.R., “Brittle fracture of adhesive joints”, International Journal of Fracture, 1992, Vol. 58(2), PP 93–114.
6. Barenblatt, G. I., “The Formation of Equilibrium Cracks during Brittle Fracture. General Ideas and Hypothesis, Axisymmetrical Cracks”, 1959, PMM Journal of Applied Mathematics and Mechanics 23, 434–444.
7. Camacho, G. T., Ortiz, M., “Computational Modeling of Impact Damage in Brittle Materials”, 1996, International Journal of Solids Structures 33, 2899–2938.
8. Espinosa, H. D., Dwivedi, S., and Lu, H. C., “Modeling Impact Induced Delamination of Woven Fiber Reinforced Composites with Contact/Cohesive Laws”, 2000, Computational Methods in Applied Mechanics, Vol. 183, 259–290.
9. Espinosa, H. D., Zavattieri, P. D., Dwivedi, S., “A Finite Deformation Continuum/Discrete Model for Description of Fragmentation and Damage in Brittle Materials”, 1998, Journal of Mechanics and Physics of Solids 46, 1909–1942.
10. Foulk, J. W., Allen, D. H., Helms, K. L. E., “Formulation of a Three-dimensional Cohesive Zone Model for Application to a Finite Element Algorithm”, 2000, Computational Methods in Applied Mechanics. Vol. 183, 51–66.
11. Geubelle, P. H., and Baylor, J., “The Impact-Induced Delamination of Laminated Composites: A 2D Simulation”, 1998, Composites, Part B, 29B, 589–602.

12. Goglio, L., Rossetto, M., "Ultrasonic testing of anaerobic bonded joints". 2002, Ultrasonics, Vol. 40(1–8), 205–210.
13. Kinloch, A.J., "Adhesion and adhesives, Science and Technology. Chapman & Hall, London, 1986.
14. Needleman, A., "An Analysis of Tensile Decohesion Along an Interface", 1990. Journal of Mechanics Physics of Solids, Vol. 38, 289–324.
15. Needleman, A., "A Continuum Model for Void Nucleation by Inclusion Debonding". 1987. ASME Journal of Applied Mechanics, Vol. 54, 525–531.
16. Siegmund, T., Brocks, W., "A Numerical Study on the Correlation between the Work of Separation and the Dissipation Rate in Ductile Fracture", 2000, Engineering Fracture Mechanics, 67, 139–154.
17. Tvergaard, V., and Hutchinson, J.W., "The Relation between Crack Growth Resistance and Fracture Process Parameters in Elastic-Plastic Solids". 1992, Journal of Mechanics and Physics of Solids, Vol. 40, 1377-1393.
18. Xu, X. P., and Needleman, A., "Numerical Simulation of Fast Crack Growth in Brittle Solids", Journal of Mechanics and Physics of Solids, 1994, Vol. 42, 1397–1434.
19. M. Alfano, F. Furgiuele, L. Pagnotta, and G. H. Paulino, "Analysis of Fracture in Aluminum Joints Bonded with a Bi-Component Epoxy Adhesive", Journal of Testing and Evaluation, 2010, Vol. 39 No. 2, PP 1-8
20. Parmigiani, J.P., Thouless, M.D., "The effects of cohesive strength and toughness on mixed-mode delamination of beam-like geometries", 2007, Engineering Fracture Mechanics Vol. 74, 2675–2699.
21. Leffler, K., Alfredsson, K.S., Stigh, U., "Shear behaviour of adhesive layers". 2007, International Journal of Solids and Structures, Vol. 44, 530–545.